Diversity and biogeochemical structuring of bacterial communities across the Porangahau ridge accretionary prism, New Zealand

Leila J. Hamdan[1,*]

Patrick M. Gillevet[2]

John W. Pohlman [3]

Masoumeh Sikaroodi[2]

Jens Greinert [4]

Richard B. Coffin[1]

Running Title:

Geomicrobiology of the Porangahau ridge

Key Words: Bacteria, AOM, Marine Sediment, Methane Sulfate, 454-Pyrosequencing

[1] Marine Biogeochemistry Section, Code 6114, U.S. Naval Research Laboratory, Overlook Ave. SW, Washington, DC 22375

[*] Corresponding Author: Phone: (202) 767-3364, Fax: (202) 404-8515, Email: leila.hamdan@nrl.navy.mil

[2] George Mason University, Microbiome Analysis Center, Department of Environmental Science and Policy, 10900 University Blvd., MSN 4D4 Manassas, Virginia 20110.

[3] U.S. Geological Survey, Woods Hole Coastal and Marine Science Center, 384 Woods Hole Rd., Woods Hole MA 02543

[4] Royal Netherlands Institute for Sea Research (NIOZ), Department of Marine Geology, P.O. Box 59, 1790 AB Den Burg, Texel, The Netherlands

ABSTRACT

Sediments from the Porangahau ridge, located off the northeastern coast of New Zealand, were studied to describe bacterial community structure in conjunction with differing biogeochemical regimes across the ridge. Low diversity was observed in sediments from an eroded basin seaward of the ridge and the community was dominated by uncultured members of the *Burkholderiales*. *Chloroflexi/*GNS and *Deltaproteobacteria* were abundant in sediments from a methane seep located landward of the ridge. Gas-charged and organic rich sediments further landward had the highest overall diversity. Surface sediments, with the exception of those from the basin, were dominated by *Rhodobacterales* sequences associated with organic matter deposition. Taxa related to the *Desulfosarcina/Desulfococcus* and the JS1 candidates were highly abundant at the sulfate-methane transition zone (SMTZ) at three sites. To determine how community structure was influenced by terrestrial, pelagic, and *in situ* substrates, sequence data were was statistically analyzed against geochemical data (e.g., sulfate, chloride, nitrogen, phosphorous, methane, bulk inorganic and organic carbon pools) using the Biota-Environmental matching procedure. Landward of the ridge, sulfate was among the most significant structuring factors. Seaward of the ridge, silica and ammonium were important structuring factors. Regardless of the transect location, methane was the principal structuring factor on SMTZ communities.

INTRODUCTION

Coastal and deep marine sediments are among the most microbially diverse environments on Earth (Inagaki, *et al.*, 2006; Sogin, *et al.*, 2006; Biddle, *et al.*, 2008). Microorganisms are involved in all major oceanic biogeochemical cycles (Galand, *et al.*, 2010) and mediate the flux of carbon in aquatic systems (Azam, 1998). Culture independent molecular studies have provided a wealth of information on the identity of prokaryotic communities in sediments, shed light on communities in methane rich marine sediments and provided evidence for the involvement of bacteria and archaea in the anaerobic oxidation of methane (AOM) (Boetius, *et al.*, 2000; Lanoil, *et al.*, 2001; Orphan, *et al.*, 2001; Knittel, *et al.*, 2005; Inagaki, *et al.*, 2006; Hamdan, *et al.*, 2008; Pernthaler, *et al.*, 2008).

Redox conditions in methane rich sediments tend to be well characterized (Borowski, *et al.*, 1996; Burns, 1998; Kastner, *et al.*, 1998; Hoehler, *et al.*, 2000; Dickens, 2001; Haese, *et al.*, 2003; Borowski, 2004; Joye, *et al.*, 2004; Milkov, *et al.*, 2004) but by comparison, far fewer studies directly relate whole community structure and composition to local abiotic conditions (Edlund, *et al.*, 2008; Galand, *et al.*, 2010). As a result, the environmental factors which structure microbial communities remain unclear in many environments (Nunoura, *et al.*, 2009). Microbial communities are structured by physical (e.g., depth, grain size, hydrodynamics), geochemical (e.g., redox conditions, organic matter), spatial (e.g., latitude, nutrient loading), and temporal factors (e.g., season). As a result, microbial community composition in methane rich sediments may vary in different geographic regions (Inagaki, *et al.*, 2006). In the same way that methane formation is locally influenced by geological, geophysical and geochemical factors, the communities involved in methane production and oxidation are likewise regionally impacted. In contrast, microbial communities at specific redox interfaces including the sulfate-methane

transition zone (SMTZ) tend to be similar across geographic distances (Inagaki, *et al.*, 2006; Hamdan, *et al.*, 2008; Harrison, *et al.*, 2009). While similarities occur under narrowly defined conditions such as the SMTZ, composition may be variable depending on the local impact of terrestrial or pelagic organic matter deposition, natural and anthropogenic nutrient loading, and methane advection or diffusion. Thus, the question emerges as to how local heterogeneity in environmental conditions impacts microbial communities throughout the sediment column in methane influenced locations. The goals for this study were to investigate bacterial community composition in methane charged and nearby methane poor sediments on the southern Hikurangi Margin, and to correlate community composition to local abiotic factors.

In the last two decades, numerous cold seeps have been discovered on the Hikurangi Margin (Henrys, *et al.*, 2003; Faure, *et al.*, 2006; Crutchley, *et al.*, 2010; Naudts, *et al.*, 2010; Schwalenberg, *et al.*, 2010). Methane is prevalent in this region due to accelerated sediment accretion of up to 12 mm/yr (Martin, *et al.*, 2010). Fluids are expelled from subducting sediments in focused locations (Jones, *et al.*, 2010; Klaucke, *et al.*, 2010; Naudts, *et al.*, 2010; Pecher, *et al.*, 2010). These fluids often contain methane (Barnes, *et al.*, 2010) and support diverse benthic communities (Baco, *et al.*, 2010; Sommer, *et al.*, 2010; Thurber, *et al.*, 2010). Evaluations of seeps along the Hikurangi margin have focused on their geological framework (Thomsen, *et al.*, 2001; Barnes, *et al.*, 2010; Pecher, *et al.*, 2010) while others have evaluated the formaminiferal (Barnette, *et al.*, 1993; Martin, *et al.*, 2010; Thurber, *et al.*, 2010) and invertebrate diversity of chemosynthetic communities (Baco, *et al.*, 2010). Prior to the present study, however, bacterial communities had not been described. Due its geological heterogeneity and the availability of methane, pelagic and accretionary material (Barnes, *et al.*, 2010; Pecher,

et al., 2010; Schwalenberg, *et al.*, 2010), this area provides an ideal backdrop for assessing the impact of local variability on bacterial community structure.

MATERIALS AND METHODS

Regional Setting

Sampling occurred aboard the R/V *Tangaroa* (National Institute of Water and Atmospheric Research) during the TAN0607 June-July 2006 cruise on the southern Hikurangi margin. Samples were collected along a 7 km cross-Porangahau ridge transect described by Schwalenberg *et al.* (2010) and Pecher *et al.* (2010) (Figure 1). These previous studies incorporated seismic, thermal conductivity, controlled source electromagnetic (CSEM) analysis and preliminary geochemical results, and revealed a narrowly (meter scale) constrained area of methane enriched fluid advection on the landward (western) flank of the ridge. An upward bend in the bottom simulating reflector (BSR) was evident on the seaward (eastern) flank of the ridge. Across the ridge, high amplitude reflections starting at BSRs are attributed to free gas and gas hydrates in deep sediments (Crutchley, *et al.*, 2010; Pecher, *et al.*, 2010).

Sample Collection and Handling

Four cores were selected for molecular biological analysis from the 12 cores collected across the ridge. Piston cores (PC) up to 4.8 m long were collected in 2.75" I.D. polycarbonate core liners and cut in 10 cm whole round sections at 10 to 43 cm intervals. Sample collection is described in detail in Schwalenberg *et al.* (2010). Sediment plugs (3ml) were collected using polyethylene syringes with the ends cut off and transferred to 20 ml serum vials to measure headspace gas. Sterile polypropylene tubes were used to collect ~20g of sediment for molecular analysis. These were frozen at -20° C during transport and held at -70° C until analysis. Approximately 5 g of wet sediment was used for gravimetric determination of porosity.

Approximately 25 ml of pore-water was extracted from whole round sections using Reeburgh-style presses (Hamdan, *et al.*, 2008). Pore-water was frozen at -20° C until analysis.

Geochemical Analysis

Methane and ethane concentration was determined according to Hoehler *et al.* (2000) using a Shimadzu 14-A gas chromatograph (GC) and flame ionization detector (Hamdan, *et al.*, 2008; Schwalenberg, *et al.*, 2010). Methane stable carbon isotope ratios ($\delta^{13}C$) were obtained using a trace GC interfaced via a GC-C III combustion unit to a Delta Plus XP Isotope Ratio Mass Spectrometer (IRMS) (ThermoElectron). Measured values were plotted against reported $\delta^{13}C$ values to generate a normalization equation which was applied to reference data to the Vienna Peedee Belemnite scale. Data are expressed in the standard δ-notation as ‰.

Dissolved inorganic carbon (DIC) concentration was measured using a UIC coulometer (Hamdan, *et al.*, 2008). A Phosphoric acid - $CuSO_4$ solution was used to convert DIC to carbon dioxide and precipitate dissolved sulfides. For DIC $\delta^{13}C$ analysis, DIC was converted to carbon dioxide as above without $CuSO_4$. Separation occurred on the trace GC equipped with a Porapak-Q column and DIC $\delta^{13}C$ were measured and reported as described for methane.

Dissolved organic carbon (DOC) concentration was determined by wet chemical oxidation on an OI Analytical 1010 as described in Osburn and St. Jean (2007). DOC $\delta^{13}C$ were determined in-line on the Delta-Plus XP IRMS.

Total inorganic (TIC) and total organic carbon (TOC) were analyzed in sediments using a Fisons EA 1108 interfaced with the Delta-Plus XP IRMS. Samples were analyzed first for total carbon (TC), and then for TOC after addition of 10% HCl. Mass balance approaches were used to calculate TIC weight percent (wt %) and stable carbon isotopes ($\delta^{13}C_{TIC}$) with the equations:

(**1**) $\%TIC = \%TC - \%TOC$ and (**2**) $\delta^{13}C_{TIC} = (\%TC \times \delta^{13}C_{TC} - \%TOC \times \delta^{13}C_{TOC}) / \%TC$

Sulfate and chloride concentrations were measured with a Dionex DX-120 ion chromatograph equipped with a 4-mm AS-9HC column (Paull, *et al.*, 2005). Dissolved ammonia, phosphate and silica were analyzed by the spectrophotometric methods of Grasshoff *et al.* (1983). Total dissolved sulfides (TDS) were determined according to Cline (1969).

Multitag Pyrosequencing and Phylogenetic Analysis

Genomic DNA was extracted from ~500 mg of wet sediment using the Bio 101 FastDNA® SPIN kit for soil. DNA was quantitated on a 1% agarose gel with ethidium bromide and diluted with DPEC water such that ~10 ng of DNA was used as template for PCR.

Prior to multitag pyrosequencing (MTPS), triplicate samples were analyzed by Length Heterogeneity-PCR (LH-PCR) as a quality control for linear amplification of the community and to normalize PCR yield for samples prior to pooling. Hamdan *et al.* (2008) provides a detailed description of LH-PCR. Briefly, amplification of variable regions V1 and V2 of the small subunit rRNA gene was performed using the primers 6-FAM-27F and 355R. Controls accompanied reactions to determine PCR efficiency and calibrate yield. PCR mixtures consisted of 1X Gold buffer, 2.5 mM $MgCl_2$, 0.2 mM dNTPs, 0.5U AmpliTaq Gold, 0.5 µM primers, 0.01% BSA, and DEPC water. PCR was performed on a GeneAmp 9700 (Applied Biosystems) programmed thusly: initial denaturation at 95ºC for 11 min., 35 cycles of 95ºC (30 sec), 48ºC (30 sec), 72ºC (2 min plus 5 sec per cycle), and final extension at 72 ºC (30 min). Product was visualized on an agarose gel, diluted based on product intensity, mixed with ILS-600 (Promega) and HiDi formamide, and analyzed on a SpectruMedix SCE9610 capillary sequencer.

Forty-eight forward fusion primers (27F) tagged on the 5’ end with a 7 base barcode along with the emulsion PCR A adapter were used with a reverse fusion primer (355R) and emulsion PCR B adapter for MTPS. PCR was performed using these barcoded primer sets.

Samples were amplified for 30 cycles as above with a 10 minute final extension step. Tagged samples were normalized by yield, pooled, and used in the emulsion step of 454-pyrosequencing. Sequencing was performed on a GS-FLX instrument in a single slot of a 4 well gasket. The length of sequences averaged 262 bp. The sequence analysis pipeline is described Naqvi *et al.* (2010). Briefly, sequences shorter than 75 bp, with quality scores less than 25 and those with multiple Ns were removed before analysis. Sequences were assigned to samples based on barcodes. Operational taxonomic units (OTUs) were clustered using CD-HIT and phylotypes were assigned to OTUs using MEGABLAST searches against GenBank. The abundance of each phylotype (taxa) was annotated using the number of reads in each OTU and relative abundance was calculated using the total number of reads from each barcode. MEGABLAST searches were conducted using a minimum cutoff of 96%, e-value of 10^{-9}, bit size of 60 and word size of 50. This resulted in 95% of sequences producing significant hits. An additional layer of filtering was used to sort results by % identity, bit-score and coverage of alignment. A custom PERL script parsed out two hits per sequence: the one with the highest match, and the one with the highest match containing phylogenetic information. The hit with the highest match is reported, however this approach provides helpful information for environmental studies which generate a large number of sequences related to unidentified environmental phylotypes.

Statistical Analysis

Primer v6 (Plymouth Marine Laboratories) was used for all statistical analyses. Phylotype diversity was estimated using the Simpson's Index (D). A Bray-Curtis similarity matrix was constructed for MTPS data and evaluated at $\rho = 0.05$. Non-metric multi-dimensional scaling (MDS) and hierarchal cluster analysis were conducted on MTPS similarity data to graphically display sample assemblages. The minimum stress level for the analysis was 0.01

with 25 restarts. MTPS similarity data were applied to the Biota and Environment (Bio-Env) matching procedure to determine which abiotic factors could be attributed with structuring communities (Clarke & Ainsworth, 1993; Clarke & Warwick, 2006; Hamdan, *et al.*, 2008). The analysis generates a Spearman rank correlation coefficient (ρ), to explain covariance between data sets and attributes covariance to geochemical variables. A ρ near zero indicates limited covariance and ρ near one indicates strong covariance.

RESULTS

Sediment Geochemistry

PC4 and PC17 were landward (west) of the ridge (Figure 1). In PC4, methane and ethane were near the limits of detection (LOD) except at depth (Figures 2A and 2B). TOC and TIC wt% moderately decreased (Figures 2C and 2E) and DOC concentration increased (Figure 2D) with depth in PC4. DIC concentration increased from <5 mM to a maximum of 20 mM between 200 and 430 cmbsf (Figure 2F). Sulfate concentration decreased from 26 mM, to the LOD in the same depth range (Figure 3A). The TDS maximum in PC4 was concomitant with the DIC maximum (Figure 3B). Chloride concentration showed no depth dependent trends (Figure 3C). Silica, ammonium and phosphate concentration increased (Figure 3D, 3E and 3F) and porosity decreased (Figure 3G) with depth in PC4. The SMTZ was determined as the depth where sulfate and methane approached the LOD. The SMTZ in PC4 was at 405 cmbsf. At the SMTZ, methane and DIC were ^{13}C-depleted compared to depths above and below (Table 1).

Although PC17 was the shallowest core, methane and ethane concentrations were highest (overall) at its base (Figure 2A). There were no depth trends for TOC or DOC in the core (Figure 2C and 2D). In PC17, a peak in TIC wt% was observed at 156 cmbsf (Figures 2E). DIC concentration increased linearly from 80 to 156 cmbsf. Minimum sulfate and maximum TDS

and silica concentrations were at 180 cmbsf in PC17 (Figure 3A, 3B and 3D). In PC17, no trend in ammonium concentration vs. depth was found; phosphate concentration increased linearly with depth (Figures 3E and 3F). Porosity in PC17 was reduced compared to PC4 (Figure 3G). The depth of the SMTZ in PC17 was 156 cmbsf. At the SMTZ methane, TOC, DOC and TIC were ^{13}C-depleted compared to other depths (Table 1) and carbonate deposits were evident.

PC7 and PC14 were seaward (west) of the ridge (Figure 1). In PC7, maximum methane concentration was at the core base. Ethane was not detected in either seaward core. The lowest average TOC (Figure 2C) and highest average TIC were in PC7 (Figure 2E). A peak in TIC was observed from 190 to 240 cmbsf in PC7. DOC and DIC concentration increased below 100 cmbsf in PC7 (Figure 2D and 2F). Sulfate concentration remained constant in the upper 100 cm of PC7 and a linear decline in concentration was observed between 100 and 200 cmbsf (Figure 3A). TDS concentration was elevated between 115 and 140 cmbsf and peaked at the core base (Figure 3B). Chloride concentration in PC7 was reduced at 215 cmbsf, the SMTZ depth (Figure 3C). Due to low pore-water volume no data for silica, phosphate or ammonium were available below 115 for PC7. In near surface samples silica concentration and porosity were significantly lower than elsewhere (Figures 3D and 3G). At the top of PC7, ammonium concentration was equal to other cores; at greater depth it was consistently higher (Figure 3E). At the SMTZ in PC7 methane and TIC and DOC were ^{13}C-depleted (Table 1).

Methane was at the LOD in PC14 (Figure 2A) and the highest average TOC was observed (Figure 2C). DOC and DIC concentration increased gradually with depth between ~200 and 322 cmbsf in PC14 (Figures 2D and 2F). In PC14, sulfate concentrations were near 28 mM in the upper ~ 200cm of the core and declined gradually towards the base. TDS concentration increased moderately in the same depth range (Figure 3B). In PC14, silica, ammonium and

phosphate concentrations increased (Figure 3D, 3E and 3F) and porosity declined moderately with depth. The SMTZ was not encountered in PC14.

MTPS Results

In total, 40144 sequences and ~10 Mb of data were obtained. On average, 836 sequences per sample were analyzed with ~220 phylotypes per sample. The Simpson's Diversity Index did not reveal statistically significant trends in numeric diversity with depth or among cores. However, taxonomic composition varied among cores and with depth. More than 50% of sequences were associated with taxa representing < 1% of the total population. Approximately 4000 singletons were excluded from the discussion in order to simplify data presentation and because they could not be statistically correlated with environmental factors. Twelve percent of sequences could not be assigned a taxonomic identification because the best hit results were to uncultured taxa that contained no information for phylogenetic assignment. Such sequences with "no clear affiliation" were related to 587 environmental phylotypes (Table 2).

Over 20% of sequences were related to uncultured *Chloroflexi*/GNS (Table 2). The *Chloroflexi*/GNS were associated with 236 phylotypes. The majority of these were related (≥98%) to uncultured isolates from methane rich sediments from the Gulf of Mexico, Chilean margin, Peru margin, Santa Barbara basin and Sea of Okhotsk. *Chloroflexi*/GNS affiliated with *Anaerolinea* spp., *Caldilineae* spp. and *Dehalococcoides* spp. accounted for <4% of total sequences. *Proteobacteria* were highly represented in the MTPS library. Of the *Proteobacteria*, *Alphaproteobacteria* were most abundant. Diversity within the *Alphaproteobacteria* was high, and sequences corresponded to ~350 phylotypes. The majority of these had no cultured relatives; 25% were related to the order *Rhodobacterales*. *Betaproteobacteria* were ~9% of sequences. More than 50% of *Betaproteobacteria* were affiliated with the order *Burkholderiales.*

Epsilonproteobacteria were not well represented. *Gammaproteobacteria* and *Deltaproteobacteria* accounted for ~3% of sequences. Sequences related to the orders *Altermonadales, Legionellales, Pseudomonadales,* and *Xanthomonadales* accounted for most *Gammaproteobacteria*. The majority of *Deltaproteobacteria* were related (>96%) to uncultured environmental isolates. Sequences related to the JS1 candidate division accounted for 17% of the library. Such sequences corresponded to 59 phylotypes, the majority of which originated from seeps and mud volcanoes in the Mediterranean Sea, Japan trench, Gulf of Mexico, Chilean margin, Peru margin, Santa Barbara basin, and South China Sea. *Bacilli*, *Bacteroidetes, Clostridia*, *Firmicutes*, *Fusobacteria,* OP8 candidates, *Planctomyceates* and *Spirochaetes* were in low abundance, but accounted for up to 14% of sequences in individual samples (Figure 4).

Chloroflexi/GNS were the most abundant group in PC4 and accounted for greater than 20% of sequences. However, at depths less than 80 cmbsf and at the SMTZ, the abundance of *Chloroflexi*/GNS was reduced (Figure 4A). *Alphaproteobacteria* sequences were also abundant in PC4. Near the surface of the core, *Alphaproteobacteria* accounted for >50% of total sequences, and abundance declined with depth. By contrast, the abundance of JS1 candidates and *Betaproteobacteria* increased with depth in this core.

In PC17, *Chloroflexi*/GNS and *Alphaproteobacteria* sequences were most abundant near the top of the core and declined with depth. Like PC4, JS1 candidates and *Betaproteobacteria* were abundant at the core base (Figure 4B). PC17 had the highest concentration of *Deltaproteobacteria* overall. *Deltaproteobacteria* were ~7% of sequences in PC17 and were concentrated at the SMTZ, and at the top of the core. *Deltaproteobacteria* in PC17 were largely related to the order *Desulfobacterales. Desulfosarcina/Desulfococcus* isolates from the SMTZ in

seeps on the Chilean margin (Hamdan *et al.* 2008) and Santa Barbara basin (Harrison et al 2009) were similar (≥98%) to sequences from this study.

Chloroflexi/GNS were ~43% of sequences in shallow sections of PC7 (Figure 4C); below 90 cmbsf their abundance was reduced. In contrast to other cores, *Alphaproteobacteria* sequences were minimal in PC7. *Betaproteobacteria* were concentrated at mid depths in PC7. At 140 cmbsf in PC7, *Betaproteobacteria* accounted for greater than 60% of sequences. The largest accumulation of *Gammaproteobacteria* was in the upper 200 cm of PC7. A peak in JS1 candidate and *Deltaproteobacteria* sequences were observed at the SMTZ in PC7.

Chloroflexi/GNS sequence abundance was reduced in PC14 compared to other cores (Figure 4D). *Alphaproteobacteria* and *Betaproteobacteria* accounted for ≥10% of sequences at all depths. As was the case at PC4, PC7 and PC17, JS1 candidate abundance generally increased with depth. Unclassified *Deltaproteobacteria* accounted for ~10% of sequences at the top of PC14 but were less than ~2% of sequences at other depths.

Bio-Env Matching Analysis of MTPS and Geochemical Data

The MDS plot revealed three clusters in the data set (Figure 5). One cluster was composed of samples from PC7 (PC7 cluster). Samples 7_65 to 7_66 obtained near the top of PC7 clustered with most samples from PC4, PC14 and PC17 (Main cluster). The third cluster contained the SMTZ samples from PC4 and PC7 (SMTZ cluster). The SMTZ sample from PC17 (17-137) was a near outlier of this group. The Bio-Env matching analysis was used to describe abiotic factors responsible for clustering of samples (Table 3). In landward cores PC4 and PC17, sulfate was an important structuring factor. In PC4, DIC also yielded a ρ value >0.63. In PC17, sulfate, TDS, methane and silica all yielded ρ values > 0.70. In the seaward core PC7, sulfate was the only variable which yielded a $\rho > 0.50$. In PC14 also seaward of the ridge, silica

and ammonium yielded ρ values of 0.55 and 0.44 respectively. The Bio-Env analysis was conducted on the sample clusters identified in the MDS plot (Figure 5; Table 3). In order to improve the statistical relevance of the analysis, included in the SMTZ were two additional samples which were ordinates to the cluster (17_137 and 17_138). In the Main cluster, silica and TOC yielded the highest ρ values. TIC provided the highest ρ value for the PC7 cluster, For the SMTZ cluster, the variable with greatest covariance with MTPS data was methane ($\rho = 0.68$).

DISCUSSION

Factors Structuring Bacterial Communities

Geological and geochemical conditions of the sedimentary environment play an important role in bacterial community structure and diversity (Kuehl, *et al.*, 1996; Edlund, *et al.*, 2008). Likewise, availability of organic carbon and methane at each site likely drives bacterial diversity. With the exception of the PC7 cluster (Figure 5), there were no distinct separations of communities based on location alone. However, different abiotic factors were attributed as influences on community structure in each core and in each MDS cluster.

PC7 Cluster

The central question of this study was determining the influence of local environmental heterogeneity on bacterial community composition. Local influence was best demonstrated at PC7. The features that delineated the PC7 cluster were minimal *Alphaproteobacteria* and elevated *Betaproteobacteria* sequences (Figure 4B). Samples in the PC7 cluster had high concentration of *Betaproteobacteria* (Figure 5) associated with the order *Burkholderiales*, and genus *Achromobacter*. Such sequences were 99% similar to two cultured isolates of *Achromobacter insolitus* (GenBank Accession EU221379 and EU520399). In laboratory experiments, these isolates exhibited diazotrophism (Sala, *et al.*, 2008) and synthesis of the

enzyme 1-aminocyclopropane-1-carboxylate (ACC) deaminase which is responsible for hydrolysis of the ethylene precursor ACC into ammonia and a-ketobutyrate. Common to these isolates is the capacity to generate ammonium. The presence of sequences related to isolates described above may explain elevated ammonium concentrations in PC7 relative to other cores (Figure 3E) and suggest a biological pathway for ammonium generation. The geochemical data support a hypothesis of *in situ* ammonium production in PC7. In PC7, % nitrogen (not shown) averaged 0.05, approximately half that observed elsewhere. Average TOC wt% was reduced compared to other locations, and C: N ratios were <6.2 compared to an average of 7.6 at other sites. Surface porosity (Figure 3G) and dissolved silica concentrations were reduced in the upper 100 cm of PC7 relative to other cores (Figure 3D). Dissolved silica may be used as an indicator of phytodetritus deposition because its concentration in sediment is controlled by burial and dissolution of silicate (Schink, *et al.*, 1974; Schink, *et al.*, 1975; Demaster, 1981). The depth profile shape for silica in PC7 was similar to other cores although surface concentrations were reduced. This suggests that controls on silica dissolution are similar across transect, but that silicate is diminished at the surface of PC7. Reduced silica, TOC, bulk nitrogen, and porosity, and low C:N ratios suggest that re-supply of organic matter and nitrogen was reduced in surface sediments at PC7. This was unexpected since basins such as the one PC7 was positioned in often act as sediment traps which could explain ammonium enrichment. However, seismic data do not suggest substantial sedimentation near PC7 (Pecher, *et al.*, 2010). Current flow is channeled down the basin (Carter & Manighetti, 2006) and causes erosion (I. Pecher, pers. comm.) which may remove surface deposition and establish a nitrogen requirement. Because some *Achromobacter* generate ammonium from nitrate under nitrate-limited conditions (King &

Nedwell, 1985), the physical conditions at PC7 may have provided advantage to *A. insolitus* related taxa and may explain their elevated sequence abundance.

Other studies have demonstrated *in situ* nitrogen production in methane rich marine sediments. Dekas *et al.* (2009) documented diazotrophism in aggregates of ANME-2 and *Desulfosarcina/Desulfococcus*. Further study may reveal if diazotrophism, ACC cleavage or other microbial nitrogen cycling partnerships occur in these sediments.

Main Cluster

The Main cluster included most samples from PC4, PC17 and PC14. In these cores, *Alphaproteobacteria* were abundant near the surface, and declined with depth (Figure 4A, 4C and 4D). Others report similar depth trends for this group in marine sediments (Webster, *et al.*, 2006; Mills, *et al.*, 2008). The most abundant *Alphaproteobacteria* in the Main cluster were 99% related to uncultured isolates from organic rich surface sediments near the Crozet Island archipelago (GenBank accession FM214379 and FM214399). These phylotypes accounted for 26% of *Alphaproteobacteria* in this study, were observed in nearly all sample from the Main cluster, and were absent from PC7. *Rhodobacterales* accounted for most *Alphaproteobacteria* with known phylogeny. The most abundant *Rhodobacterales* was associated with a *Loktanella* sp. (GenBank accession FJ196061) isolated from coastal sediments off east Antarctica. The second most abundant *Rhodobacterales* phylotype was associated with a *Rhodobacter* sp. isolate (GenBank accession EU979473) from the Columbia River estuarine turbidity maximum. *Rhodobacterales* are primary surface sediment colonizers in coastal waters (Dang & Lovell, 2000) and often play a role in oxidation of newly deposited organic matter. The Bio-Env results implicate silica and TOC as important structuring factors on the Main cluster (Table 3). These

results may explain why sequences associated organic matter utilization were so abundant in surface samples in the Main cluster.

The order *Rhizobales* was well represented in samples in the Main cluster and accounted for 9% of *Alphaproteobacteria*. *Rhizobales* related to the *Methylocystaceae* family were in highest abundance in PC4, limited in PC17 and PC14 and not observed in PC7. The elevated abundance of *Methylocystaceae* in PC4 compared to other cores suggests that although *Methylocystaceae* are methanotrophic, phylotypes in this study may proliferate under conditions of low methane concentration. In addition, anoxic conditions in PC17 and PC7 (indicated by the presence of TDS - Figure 3B) would inhibit obligately aerobic *Methylocystaceae* and may explain their reduced sequence abundance in the cores.

The *Chloroflexi*/GNS featured largely in samples from the Main cluster (Figure 5). This and other studies report that the location of *Chloroflexi*/GNS within the sediment column is variable (Inagaki, *et al.*, 2003; Kormas, *et al.*, 2003; Inagaki, *et al.*, 2006; Heijs, *et al.*, 2007; Biddle, *et al.*, 2008; Hamdan, *et al.*, 2008; Harrison, *et al.*, 2009). *Chloroflexi*/GNS are ubiquitous in methane rich sediments (Webster, *et al.*, 2006). In such sediments from the Chilean margin, Santa Barbara basin, Mediterranean Sea and Gulf of Mexico, *Chloroflexi*/GNS are most prevalent below the SMTZ (Reed, *et al.*, 2006; Heijs, *et al.*, 2007; Hamdan, *et al.*, 2008; Harrison, *et al.*, 2009). Others have discovered *Chloroflexi*/GNS to be uniformly distributed in the deep subsurface (>50 m) sediments on the Peru margin (Biddle, *et al.*, 2008). Inagaki *et al.* (2006) noted that on the Peru margin, *Chloroflexi*/GNS dominate organic-rich methane bearing sediments which lacked gas hydrates and that this was a key biological factor distinguishing nearby sites that contained gas hydrates from those that did not.

Frequent observations of *Chloroflexi*/GNS in methane rich sediments has prompted speculation on their role in methanogenesis (Sekiguchi, 2006). The semi-ubiquitous appearance of *Chloroflexi*/GNS in studies of marine sediments (Kormas, *et al.*, 2003; Biddle, *et al.*, 2008) indicate that factors other than methane are correlated with their appearance. In this study, no direct relationship between *Chloroflexi*/GNS and methane was observed. Methane concentration was generally low in samples with high *Chloroflexi*/GNS abundance, and the Bio-Env analysis (Table 4) indicated that TOC, not methane was a structuring factor on the Main cluster.

Chloroflexi/GNS were abundant in sediments from the top of PC7. In PC7 samples which grouped in the Main cluster (Figure 5) the majority of *Chloroflexi*/GNS were affiliated with isolates from the Brazos-Trinity basin of the Gulf of Mexico (Nunoura, *et al.*, 2009). The Brazos -Trinity basin like PC7 is relatively TOC poor, having C:N ratios which are non-Redfield (Gilhooly, *et al.*, 2008). The physico-chemical and biological parity between these sites suggest bacterial composition to be a highly specific indicator of abiotic conditions in marine sediments. The location where PC7 was obtained was likely eroded by hydraulic forces. Because of this, newly deposited, labile TOC would be limited at the surface. However, erosion would expose buried recalcitrant TOC. Studies demonstrate that recalcitrant TOC is responsible for the long-term survival of microorganisms in the deep subsurface (Fredrickson & Balkwill, 2006) and may explain the observations of *Chloroflexi*/GNS in this and similar environments (Inagaki, *et al.*, 2006; Biddle, *et al.*, 2008; Nunoura, *et al.*, 2009).

Although most of PC17 was nested in the Main cluster, the robust Spearman Rank correlation coefficients for the core deserve some individual discussion. Silica was the main structuring factor in PC17 (Table 3). A significant increase in silica concentration was observed below the SMTZ, concomitant with the TDS maximum (Figure 3D). Studies demonstrate silica

dissolution in conjunction with SR, AOM and carbonate precipitation (Birnbaum & Wireman, 1984; Jørgensen & Boetius, 2007; Pierre & Fouquet, 2007). Elevated silica concentration near the SMTZ in PC17 was likely a secondary result of metabolic activity. Hence, the high ρ for silica may be the result of covariance of factors rather than direct cause and effect on community structure. This is reflected in the Bio-Env results which indicate that sulfate, TDS and methane also are important correlates on community structure in PC17 due to their coupled relationships in sediment diagenesis.

SMTZ Cluster

The biological features common to the SMTZ were elevated concentration of *Deltaproteobacteria* and JS1 candidate sequences relative to other depths (Figure 4). The most abundant JS1 phylotype in this study was ≥98% similar to an isolate from hydrate bearing sediments from the Chilean margin (GenBank Accession EF093942). The Bio-Env analysis indicated that methane was the main abiotic driver on the SMTZ cluster. Although the biogeochemical role of JS1 candidates is unknown, it has been suggested that their abundance is controlled by the presence of methane (Webster, *et al.*, 2006) and low sulfate concentration (Parkes, *et al.*, 2007). In this study, the influence of methane on JS1 candidates cannot be ruled out since they were abundant in methane rich sections of PC4, PC7 and PC17 (Figure 4). However, because they were observed in PC14 (Figure 4C), where methane was below the LOD, other factors must influence their presence. Similarly, if methane principally governed JS1 candidate abundance, it is expected that they would be most abundant in PC17 which had the highest methane concentrations; however, this was not the case. JS1 candidates are often observed in gas hydrate containing sediments (Inagaki, *et al.*, 2006) although, none were

observed in this study. The distribution of JS1 candidates in this study suggests metabolic diversity in this group, which involves more than methane metabolism.

At the SMTZ *Deltaproteobacteria* were largely affiliated with the *Desulfosarcina/Desulfococcus* subgroup. Other studies report enrichment of this subgroup at the SMTZ (Mills, *et al.*, 2003; Inagaki, *et al.*, 2006; Hamdan, *et al.*, 2008) and on their suspected role in AOM. The appearance of these sequences outside of the SMTZ was limited, indicating that conditions at the SMTZ select for these phylotypes. Below the SMTZ, *Deltaproteobacteria* generally accounted for < 1% of sequences. Above, phylotypes related 98% to a *Desulfobacter* isolate (GenBank Accession U85476) obtained from salt marsh sediments were abundant. The high concentration of *Desulfobacterales* - the order which encompasses most marine sulfate reducers, above the SMTZ is indicative of the SR zone (Arakawa, *et al.*, 2006).

The data for *Deltaproteobacteria* indicate that sulfate dependent AOM and organoclastic SR likely occurred in cores from this study. Without a conservative tracer to differentiate physical mixing from biogeochemical processes, it is difficult to delineate SR processes (i.e., organoclastic SR vs. AOM) from the non-linear sulfate profiles (Pohlman, *et al.*, 2008). However, sulfate and methane profiles, particularly from PC7 and PC17, the shallow depth of the SMTZ in these cores, and concentration of *Desulfosarcina/Desulfococcus* related sequences suggest that SR associated with AOM was focused at the SMTZ.

Methane, DIC, TOC and DOC $\delta^{13}C$ (Table 1) and methane and sulfate concentration data support the idea that both AOM and organoclastic SR impact sediment biogeochemistry in PC4, PC17 and PC7. TOC $\delta^{13}C$ above the SMTZ in these cores fall within the range of pelagic organic matter (Claypool & Kaplan, 1974; Peterson, *et al.*, 1994; Niggemann & Schubert, 2006). Thus, above the SMTZ ^{13}C-enriched DIC may have resulted from metabolism of pelagic organic

matter. However, at the SMTZ of PC4 and PC17 ^{13}C-depleted DIC could only result from oxidation of ^{13}C-depleted methane since δ^{13}C for TOC and DOC in these cores cannot explain the substantially ^{13}C-depleted DIC. At the SMTZ in PC7 and PC17, TIC concentration was elevated relative to PC4 and PC14 (Figure 2E) and carbonate deposits were observed in PC17. Reduced porosity at the SMTZ was observed in both PC17 and PC7. These observations suggest carbonate precipitation in conjunction with AOM. In PC17, ^{13}C-depleted TIC at the SMTZ can only be explained by AOM (Table 1). DOC δ^{13}C indicate that ^{13}C-depleted methane was incorporated into the organic carbon pool at the SMTZ of PC17 (Table 1). TIC and DOC were both ^{13}C-depleted at the SMTZ in PC7 (Table 1). Neither TIC accumulation nor TIC ^{13}C-depletion was observed in PC4, however, ^{13}C-depleted DIC was (Table 1). Because the abundance of *Desulfosarcina/Desulfococcus* at the SMTZ in PC4 was reduced compared to PC17 and PC7, this may be indicative of lower rates of AOM, and hence, a less distinct geochemical signature. However, the reduced supply of methane at PC4 relative to PC17 and PC7 may have driven the reduction in *Desulfosarcina/Desulfococcus* in the first place. As a whole, these data suggest that the local influence of methane on bacterial communities is significant in PC17 and PC7, reduced in PC4, and negligible in PC14.

CONCLUSIONS

Geomicrobial studies which incorporate large geochemical datasets in conjunction with next generation sequencing assist in understanding the biogeochemical role of uncultured bacterial populations. In methane seep sediments, much uncertainly remains as to the role of *Chloroflexi*/GNS and JS1 candidates. Their frequent appearance in such environments has resulted in the expectation that methane is correlated with their appearance. However, statistical analysis indicates that TOC may be an important structuring factor on *Chloroflexi/GNS.* Methane

likely influences the presence of many JS1 candidates, however because of their appearance in methane poor locations, other substrates must be used as metabolites by this group. Heterogeneity in the supply of nutrients and the composition of carbon pools across the ridge is associated with geophysical, hydrodynamic and geological features. Such heterogeneity is reflected in the composition of microbial communities. In some cases heterogeneity may be the result of metabolic activity by different communities. However, at the SMTZ a somewhat homogeneous bacterial population was evident and community structure bore similar characteristics to SMTZ communities observed in methane seeps throughout the ocean.

ACKNOWLEDGEMENTS

This work was supported by the Naval Research Laboratory Chemistry Division Young Investigator Program and the Office of Naval Research platform support program. We thank the captain and crew of the R/V *Tangaroa* for field assistance, Roswell Downer and Layton Bryant for sample recovery, Rebecca Plummer and Dillon Gustafson for laboratory assistance and Ingo Pecher and Suzannah Toulmin for helpful discussions. We thank Co-Chief Scientists Ingo Pecher and Stewart Henrys and the CHARMNZ science party for their support of this study.

REFERENCES

Arakawa S, Sato T, Sato R, Zhang J, Gamo T, Tsunogai U, Hirota A, Yoshida Y, Usami R, Inagaki F & Kato C (2006) Molecular phylogenetic and chemical analyses of the microbial mats in deep-sea cold seep sediments at the northeastern Japan Sea. *Extremophiles* **10**: 311-319.

Azam F (1998) Microbial control of oceanic carbon flux: The plot thickens. *Science* **280**: 694-696.

Baco AR, Rowden AA, Levin LA, Smith CR & Bowden DA (2010) Initial characterization of cold seep faunal communities on the New Zealand Hikurangi margin. *Marine Geology* **272**: 251-259.

Barnes PM, Lamarche G, Bialas J, Henrys S, Pecher I, Netzeband GL, Greinert J, Mountjoy JJ, Pedley K & Crutchley G (2010) Tectonic and geological framework for gas hydrates and cold seeps on the Hikurangi subduction margin, New Zealand. *Marine Geology* **272**: 26-48.

Barnette KG, Glover DD, Boyd CB, Lalka D & Sarkar MA (1993) Polycyclic Aromatic Hydrocarbon (Pah) Inducible P450 Isozymes (1a1 and 1a2) and Glutathione-S-Transferase (Gst) Activity in Human Uterine Tissues. *Clinical Research* **41**: A127-A127.

Biddle JF, Fitz-Gibbon S, Schuster SC, Brenchley JE & House CH (2008) Metagenomic signatures of the Peru Margin subseafloor biosphere show a genetically distinct environment. *Proceedings of the National Academy of Sciences of the United States of America* **105**: 10583-10588.

Birnbaum SJ & Wireman JW (1984) Bacterial Sulfate Reduction and Ph - Implications for Early Diagenesis. *Chemical Geology* **43**: 143-149.

Boetius A, Ravenschlag K, Schubert CJ, Rickert D, Widdel F, Gleseke A, Amann R, Jørgensen BB, Witte U & Pfannkuche O (2000) A marine microbial consortium apparently mediating anaerobic oxidation methane. *Nature* **407**: 623-626.

Borowski WS (2004) A review of methane and gas hydrates in the dynamic, stratified system of the Blake Ridge region, offshore southeastern North America. *Chem. Geol.* **205**: 311-346.

Borowski WS, Paull CK & Ussler W (1996) Marine pore-water sulfate profiles indicate in situ methane flux from underlying gas hydrate. *Geology* **24**: 655-658.

Burns SJ (1998) Carbon isotopic evidence for coupled sulfate reduction methane oxidation in Amazon Fan sediments. *Geochimica et Cosmochimica Acta* **62**: 797-804.

Carter L & Manighetti B (2006) Glacial/interglacial control of terrigenous and biogenic fluxes in the deep ocean off a high input, collisional margin: A 139 kyr-record from New Zealand. *Marine Geology* **226**: 307-322.

Clarke KR & Ainsworth M (1993) A method of linking multivariate community structure to environmental variables. *Mar. Ecol. Prog. Ser.* **92**: 205-219.

Clarke KR & Warwick RM (2006) Change in marine communities: An approach to statistical analysis and interpretation. ed.^eds.), p.^pp. Plymouth Marine Laboratories.

Claypool GE & Kaplan IR (1974) The origin and distribution of methane in marine sediments. *Natural Gases in Marine Sediments.*,(Kaplan IR, ed.^eds.), p.^pp. 99-139. Plenum, New York.

Cline J (1969) *Spectrophotometric determination of hydrogen sulphide in natural waters*.

Crutchley GJ, Pecher IA, Gorman AR, Henrys SA & Greinert J (2010) Seismic imaging of gas conduits beneath seafloor seep sites in a shallow marine gas hydrate province, Hikurangi Margin, New Zealand. *Marine Geology* **272**: 114-126.

Dang H & Lovell CR (2000) Bacterial Primary Colonization and Early Succession on Surfaces in Marine Waters as Determined by Amplified rRNA Gene Restriction Analysis and Sequence Analysis of 16S rRNA Genes. *Applied and Environmental Microbiology* **66**: 467-475.

Dekas AE, Poretsky RS & Orphan VJ (2009) Deep-Sea Archaea Fix and Share Nitrogen in Methane-Consuming Microbial Consortia. *Science* **326**: 422-426.

Demaster DJ (1981) The Supply and Accumulation of Silica in the Marine-Environment. *Geochimica et Cosmochimica Acta* **45**: 1715-1732.

Dickens GR (2001) Sulfate profiles and barium fronts in sediment on the Blake Ridge: Present and past methane fluxes through a large gas hydrate reservoir. *Geochimica et Cosmochimica Acta* **65**: 529-543.

Edlund A, Hårdeman F, Jansson JK & Sjöling S (2008) Active bacterial community structure along vertical redox gradients in Baltic Sea sediment. *Environmental Microbiology* **10**: 2051-2063.

Faure K, Greinert J, Pecher IA, Graham IJ, Massoth GJ, De Ronde CEJ, Wright IC, Baker ET & Olson EJ (2006) Methane seepage and its relation to slumping and gas hydrate at the Hikurangi margin, New Zealand. *New Zealand Journal of Geology and Geophysics* **49**: 503-516.

Fredrickson JK & Balkwill DL (2006) Geomicrobial Processes and Biodiversity in the Deep Terrestrial Subsurface. *Geomicrobiology Journal* **23**: 345-356.

Galand PE, Potvin M, Casamayor EO & Lovejoy C (2010) Hydrography shapes bacterial biogeography of the deep Arctic Ocean. *ISME J* **4**: 564-576.

Gilhooly W, Macko SA & Flemings PB (2008) Data report: Isotope compositions of sedimentary organic carbon and total nitrogen from Brazos-Trinity Basin IV (Sites U1319 and U1320) and Ursa Basin (Sites U1322 and U1324), deepwater Gulf of Mexico. *Proceedings of the Intergrated Ocean Drilling Program* **208**: 1-11.

Grasshoff K, Ehrhardt M, Kremling K & Almgren T (1983) *Methods of seawater analysis*. Verlag Chemie, Weinheim.

Haese RR, Meile C, Van Cappellen P & De Lange GJ (2003) Carbon geochemistry of cold seeps: Methane fluxes and transformation in sediments from Kazan mud volcano, eastern Mediterranean Sea. *Earth Planet. Sci. Let.* **212**: 361-375.

Hamdan LJ, Gillevet PM, Sikaroodi M, Pohlman JW, Plummer RE & Coffin RB (2008) Geomicrobial characterization of gas hydrate-bearing sediments along the mid-Chilean margin. *Fems Microbiology Ecology* **65**: 15-30.

Harrison BK, Zhang H, Berelson W & Orphan VJ (2009) Variations in Archaeal and Bacterial Diversity Associated with the Sulfate-Methane Transition Zone in Continental Margin Sediments (Santa Barbara Basin, California). *Applied and Environmental Microbiology* **75**: 1487-1499.

Heijs S, Haese R, van der Wielen P, Forney L & van Elsas J (2007) Use of 16S rRNA Gene Based Clone Libraries to Assess Microbial Communities Potentially Involved in Anaerobic Methane Oxidation in a Mediterranean Cold Seep. *Microbial Ecology* **53**: 384-398.

Henrys SA, Ellis S & Uruski C (2003) Conductive heat flow variations from bottom-simulating reflectors on the Hikurangi margin, New Zealand. *Geophysical Research Letters* **30**: -.

Hoehler TM, Borowski WS, Alperin MJ, Rodriguez NM & Paull CK (2000) Model, stable isotope, and radiotracer characterization of anaerobic methane oxidation in gas hydrate-bearing sediments of the Blake Ridge. *Proc. Ocean Drilling Prog.: Sci. Results* **164**: 79-85.

Inagaki F, Suzuki M, Takai K, Oida H, Sakamoto T, Aoki K, Nealson KH & Horikoshi K (2003) Microbial communities associated with geological horizons in coastal subseafloor sediments from the Sea of Okhotsk. *Applied and Environmental Microbiology* **69**: 7224-7235.

Inagaki F, Nunoura T, Nakagawa S, Teske A, Lever M, Lauer A, Suzuki M, Takai K, Delwiche M, Colwell FS, Nealson KH, Horikoshi K, D'Hondt S & Jorgensen BB (2006) Biogeographical distribution and diversity of microbes in methane hydrate-bearing deep marine sediments, on the Pacific Ocean Margin. *Proc. Natl. Acad. Sci. U.S.A.* **103**: 2815-2820.

Jones AT, Greinert J, Bowden DA, Klaucke I, Petersen CJ, Netzeband GL & Weinrebe W (2010) Acoustic and visual characterisation of methane-rich seabed seeps at Omakere Ridge on the Hikurangi Margin, New Zealand. *Marine Geology* **272**: 154-169.

Jørgensen BB & Boetius A (2007) Feast and famine - microbial life in the deep-sea bed. *Nat Rev Micro* **5**: 770-781.

Joye SB, Boetius A, Orcutt BN, Montoya JP, Schulz HN, Erickson MJ & Lugo SK (2004) The anaerobic oxidation of methane and sulfate reduction in sediments from Gulf of Mexico cold seeps. *Chemical Geology* **205**: 219-238.

Kastner M, Kvenvolden KA & Lorenson TD (1998) Chemistry, isotopic composition, and origin of a methane-hydrogen sulfide hydrate at the Cascadia subduction zone. *Earth Planet. Sci. Let.* **156**: 173-183.

King D & Nedwell DB (1985) The influence of nitrate concentration upon the end-products of nitrate dissimilation by bacteria in anaerobic salt marsh sediment. *FEMS Microbiology Letters* **31**: 23-28.

Klaucke I, Weinrebe W, Petersen CJ & Bowden D (2010) Temporal variability of gas seeps offshore New Zealand: Multi-frequency geoacoustic imaging of the Wairarapa area, Hikurangi margin. *Marine Geology* **272**: 49-58.

Knittel K, Lösekann T, Boetius A, Amann R & Kort R (2005) Diversity and distribution of methanotrophic archaea at cold seeps. *Applied and Environmental Microbiology* **71**: 467-479.

Kormas KA, Smith DC, Edgcomb V & Teske A (2003) Molecular analysis of deep subsurface microbial communities in Nankai Trough sediments (ODP Leg 190, Site 1176). *FEMS Microbiology Ecology* **45**: 115-125.

Kuehl SA, Nittrouer CA, Allison MA, Ercilio L, Faria C, Dukat DA, Jaeger JM, Pacioni TD, Figueiredo AG & Underkoffler EC (1996) Sediment deposition, accumulation, and seabed dynamics in an energetic fine-grained coastal environment. *Continental Shelf Research* **16**: 787-815.

Lanoil BD, Sassen R, La Duc MT, Sweet ST & Nealson KH (2001) Bacteria and archaea physically associated with Gulf of Mexico gas hydrates. *Applied and Environmental Microbiology* **67**: 5143-5153.

Martin RA, Nesbitt EA & Campbell KA (2010) The effects of anaerobic methane oxidation on benthic foraminiferal assemblages and stable isotopes on the Hikurangi Margin of eastern New Zealand. *Marine Geology* **272**: 270-284.

Milkov AV, Vogt PR, Crane K, Lein AY, Sassen R & Cherkashev GA (2004) Geological, geochemical, and microbial processes at the hydrate-bearing Haakon Mosby mud volcano: A review. *Chem. Geol.* **205**: 347-366.

Mills HJ, Hodges C, Wilson K, MacDonald IR & Sobecky PA (2003) Microbial diversity in sediments associated with surface-breaching gas hydrate mounds in the Gulf of Mexico. *FEMS Microbiology Ecology* **46**: 39-52.

Mills HJ, Hunter E, Humphrys M, Kerkhof L, McGuinness L, Huettel M & Kostka JE (2008) Characterization of Nitrifying, Denitrifying, and Overall Bacterial Communities in Permeable Marine Sediments of the Northeastern Gulf of Mexico. *Applied and Environmental Microbiology* **74**: 4440-4453.

Naqvi A, Rangwala H, Spear G & Gillevet P (2010) Analysis of Multitag Pyrosequence Data from Human Cervical Lavage Samples. *Chemistry & Biodiversity* **7**: 1076-1085.

Naudts L, Greinert J, Poort J, Belza J, Vangampelaere E, Boone D, Linke P, Henriet J-P & De Batist M (2010) Active venting sites on the gas-hydrate-bearing Hikurangi Margin, off New Zealand: Diffusive- versus bubble-released methane. *Marine Geology* **272**: 233-250.

Niggemann J & Schubert CJ (2006) Fatty acid biogeochemistry of sediments from the Chilean coastal upwelling region: Sources and diagenetic changes. *Org. Geochem.* **37**: 626-647.

Nunoura T, Soffientino B, Blazejak A, Kakuta J, Oida H, Schippers A & Takai K (2009) Subseafloor microbial communities associated with rapid turbidite deposition in the Gulf

of Mexico continental slope (IODP Expedition 308). *FEMS Microbiology Ecology* **69**: 410-424.

Orphan VJ, Hinrichs KU, Ussler Iii W, Paull CK, Taylor LT, Sylva SP, Hayes JM & Delong EF (2001) Comparative analysis of methane-oxidizing archaea and sulfate-reducing bacteria in anoxic marine sediments. *Applied and Environmental Microbiology* **67**: 1922-1934.

Osburn CL & St-Jean G (2007) The use of wet chemical oxidation with high-amplification isotope ratio mass spectrometry (WCO-IRMS) to measure stable isotope values of dissolved organic carbon in seawater. *Limnology and Oceanography-Methods* **5**: 296-308.

Parkes RJ, Cragg BA, Banning N, Brock F, Webster G, Fry JC, Hornibrook E, Pancost RD, Kelly S, Knab N, Jørgensen BB, Rinna J & Weightman AJ (2007) Biogeochemistry and biodiversity of methane cycling in subsurface marine sediments (Skagerrak, Denmark). *Environmental Microbiology* **9**: 1146-1161.

Paull CK, Ussler Iii W, Lorenson T, Winters W & Dougherty J (2005) Geochemical constraints on the distribution of gas hydrates in the Gulf of Mexico. *Climate Dynamics* **25**: 273-280.

Pecher IA, Henrys SA, Wood WT, Kukowski N, Crutchley GJ, Fohrmann M, Kilner J, Senger K, Gorman AR, Coffin RB, Greinert J & Faure K (2010) Focussed fluid flow on the Hikurangi Margin, New Zealand -- Evidence from possible local upwarping of the base of gas hydrate stability. *Marine Geology* **272**: 99-113.

Pernthaler A, Dekas AE, Brown CT, Goffredi SK, Embaye T & Orphan VJ (2008) Diverse syntrophic partnerships from-deep-sea methane vents revealed by direct cell capture and metagenomics. *Proceedings of the National Academy of Sciences of the United States of America* **105**: 7052-7057.

Peterson B, Fry B, Hullar M, Saupe S & Wright R (1994) The Distribution and Stable Carbon Isotopic Composition of Dissolved Organic-Carbon in Estuaries. *Estuaries* **17**: 111-121.

Pierre C & Fouquet Y (2007) Authigenic carbonates from methane seeps of the Congo deep-sea fan. *Geo-Marine Letters* **27**: 249-257.

Pohlman JW, Ruppel C, Hutchinson DR, Downer R & Coffin RB (2008) Assessing sulfate reduction and methane cycling in a high salinity pore water system in the northern Gulf of Mexico. *Marine and Petroleum Geology* **25**: 942-951.

Reed A, Lutz R & Vetriani C (2006) Vertical distribution and diversity of bacteria and archaea in sulfide and methane-rich cold seep sediments located at the base of the Florida Escarpment. *Extremophiles* **10**: 199-211.

Sala VMR, Cardoso EJBN, Garboggini FF, Nogueira ND & da Silveira APD (2008) Achromobacter insolitus and Zoogloea ramigera associated with wheat plants (Triticum aestivum). *Biology and Fertility of Soils* **44**: 1107-1112.

Schink DR, Fanning KA & Pilson MEQ (1974) Dissolved Silica in Upper Pore Waters of Atlantic Ocean-Floor. *Journal of Geophysical Research* **79**: 2243-2250.

Schink DR, Guinasso NL & Fanning KA (1975) Processes Affecting Concentration of Silica at Sediment-Water Interface of Atlantic Ocean. *Journal of Geophysical Research-Oceans and Atmospheres* **80**: 3013-3031.

Schwalenberg K, Haeckel M, Poort J & Jegen M (2010) Evaluation of gas hydrate deposits in an active seep area using marine controlled source electromagnetics: Results from Opouawe Bank, Hikurangi Margin, New Zealand. *Marine Geology* **272**: 79-88.

Schwalenberg K, Wood W, Pecher I, Hamdan L, Henrys S, Jegen M & Coffin R (2010) Preliminary interpretation of electromagnetic, heat flow, seismic, and geochemical data

for gas hydrate distribution across the Porangahau Ridge, New Zealand. *Marine Geology* **272**: 89-98.

Sekiguchi Y (2006) Yet-to-be Cultured Microorganisms Relevant to Methane Fermentation Processes. *Microbes and Environments* **21**: 1-15.

Sogin ML, Morrison HG, Huber JA, Welch DM, Huse SM, Neal PR, Arrieta JM & Herndl GJ (2006) Microbial diversity in the deep sea and the underexplored "rare biosphere". *Proc. Natl. Acad. Sci. U.S.A.* **103**: 12115-12120.

Sommer S, Linke P, Pfannkuche O, Niemann H & Treude T (2010) Benthic respiration in a seep habitat dominated by dense beds of ampharetid polychaetes at the Hikurangi Margin (New Zealand). *Marine Geology* **272**: 223-232.

Thomsen TR, Finster K & Ramsing NB (2001) Biogeochemical and molecular signatures of anaerobic methane oxidation in marine sediment. *Applied and Environmental Microbiology* **67**: 1646-1656.

Thurber AR, Kröger K, Neira C, Wiklund H & Levin LA (2010) Stable isotope signatures and methane use by New Zealand cold seep benthos. *Marine Geology* **272**: 260-269.

Webster G, Parkes RJ, Cragg BA, Newberry CJ, Weightman AJ & Fry JC (2006) Prokaryotic community composition and biogeochemical processes in deep subseafloor sediments from the Peru Margin. *FEMS Microbiology Ecology* **58**: 65-85.

TABLE LEGENDS

Table 1. Summary of stable carbon isotope ratio data for methane, dissolved inorganic carbon (DIC), total inorganic carbon (TIC), dissolved organic carbon (DOC) and total organic carbon (TOC). Data are displayed for each core individually. Depth zones reported are based on the empirically determined depth of the sulfate-methane transition zone (SMTZ). Values reported are the average for each depth zone. No SMTZ was observed in PC14, thus, data for only one depth zone is presented. Cores are listed in the table in order of position (west to east) on the Porangahau ridge transect.

Table 2. Phylogenetic community structure based on 16s rRNA bacterial MTPS analysis. All samples are included in these results.

Table 3. Bio-Env procedure results. Best variable results and best combination of variables giving yielding the largest Spearman rank correlation ρ coefficient between similarity matrices of bacterial community data and abiotic variables.

FIGURE LEGENDS

Figure 1. Study location along the Porangahau ridge.

Figure 2. Depth profiles of methane (A), ethane (B), total organic carbon (TOC) (C), dissolved organic carbon (DOC) (D), total inorganic carbon (TIC) (E) and dissolved inorganic carbon (DIC) (F) concentration in PC4, PC7, PC14 and PC17.

Figure 3. Depth profiles of sulfate (A), total dissolved sulfides (TDS) (B), chloride (C), silica (D), ammonium (E) and phosphate (F) concentration and porosity (water content) (G).

Figure 4. Phylogenetic community composition in four cores collected across the ridge. Cores are arranged according to position on the ridge. Landward cores collected west of the ridge are PC4 (A) and PC17 (B). Seaward cores collected east of the ridge are PC14 (C) and PC7 (D).

Figure 5. Multi-dimensional scaling (MDS) plot of the assemblages of MTPS sequences in each sample. Contours were generated by a hierarchal cluster analysis conducted on a Bray-Curtis analysis of similarity for MTPS data.

Table 1. Summary of stable carbon isotope ratio data for methane, dissolved inorganic carbon (DIC), total inorganic carbon (TIC), dissolved organic carbon (DOC) and total organic carbon (TOC). Data are displayed for each core individually. Depth zones reported are based on the empirically determined depth of the sulfate-methane transition zone (SMTZ). Values reported are the average for each depth zone. No SMTZ was observed in PC14, thus, data for only one depth zone is presented. Cores are listed in the table in order of position (west to east) on the Porangahau ridge transect.

Core	Depth interval (cmbsf)	Depth zone (relative to SMTZ)	n	$\delta^{13}C_{methane}$	$\delta^{13}C_{DIC}$	$\delta^{13}C_{TIC}$	$\delta^{13}C_{DOC}$	$\delta^{13}C_{TOC}$
4	0-380	Above	15	-85	-18	-1	-24	-22
4	405	SMTZ	1	-108	-39	-3	-22	-22
4	430-480	Below	3	-92	-31	-2	-23	-24
17	0-131	Above	6	-74	-22	-2	-29	-23
17	156	SMTZ	1	-98	-39	-44	-40	-25
17	181-206	Below	2	-79	-44	-7	-26	-23
14	0-322	Above	13	-75	-16	0	-23	-22
7	0-190	Above	8	-82	-16	-5	-25	-22
7	215	SMTZ	1	-91	-21	-13	-27	-22
7	240-265	Below	2	-79	-34	-9	-23	-23

Table 2. Phylogenetic community structure based on 16s rRNA bacterial MTPS analysis. All samples are included in these results.

Phylogenetic Class	% of Total
Acidobacteria	0.25%
Actinobacteria	3.60%
Alphaproteobacteria	17.55%
Bacilli	1.11%
Bacteroidetes	1.07%
Betaproteobacteria	9.32%
Chloroflexi/GNS	21.43%
Clostridia	2.38%
Cyanobacteria	0.17%
Deferribacteres	0.09%
Dehalococcoidetes	0.13%
Deltaproteobacteria	3.80%
Epsilonproteobacteria	0.06%
Erysipelotrichi	0.05%
Firmicutes	1.87%
Fusobacteria	0.17%
Gammaproteobacteria	2.78%
Gemmatimonadetes	0.09%
JS1 Candidate Division	17.23%
Nitrospirae	0.03%
No clear affiliaiton	12.42%
OD1 Candidate Division	0.01%
OP1 Candidate Division	0.15%
OP11 Candidate Division	0.49%
OP3 Candidate Division	0.05%
OP8 Candidate Division	1.64%
Planctomycetacia	0.21%
Spirochaetes	1.40%
Tenericutes	0.02%
Tracheophyta chloroplast	0.29%
Unclassified Proteobacteria	0.10%
WS3 Candidate Division	0.04%

Table 3. Bio-Env procedure results. Best variable results and best combination of variables giving yielding the largest Spearman rank correlation ρ coefficient between similarity matrices of bacterial community data and abiotic variables.

Sample group	Best variable (ρ)	Best variable combinations (ρ)
All samples	Sulfate (0.33) Ethane (0.32) TIC (0.32) TOC (0.31)	Sulfate, Phosphate, TOC, TIC (0.460)
PC4	DIC (0.65) Sulfate (0.63) Silica (0.61) Ethane (0.57)	DIC, Silica, Phosphate (0.67)
PC7*	Sulfate (0.50) Ethane (0.33) DIC (0.31) TIC (0.21)	Sulfate (0.50)
PC14	Silica (0.54) Ammonium (0.44) Phosphate (0.42) TDS (0.41)	Silica (0.54)
PC17	Silica (0.84) TDS (0.74) Methane (0.74) Sulfate (0.72)	Sulfate, TDS, Silica, TOC, TIC (0.90)
PC7 Cluster	TIC (0.59) Sulfate (0.44) Ethane (0.40) DIC (0.35)	Chloride, DIC, TIC, (0.77)
SMTZ Cluster	Methane (0.68) TIC (0.45) TOC (0.33) Phosphate (0.10)	Methane, TOC (0.72)
Main Cluster	Silica (0.34) TOC (0.32) DIC (0.22) Sulfate (0.21)	TDS, Silica, Phosphate, TOC, TIC (0.46)

Note: Abiotic variables included in the Bio-Env analysis:
Chloride, sulfate, TDS, DIC, methane, ethane, silica, phosphate, ammonium, TOC, TIC and DOC concentration and porosity. Stable isotope data were omitted because they are not entirely independent of concentration data.
* For PC7, silica, phosphate and ammonium were omitted from this analysis because of incomplete data sets

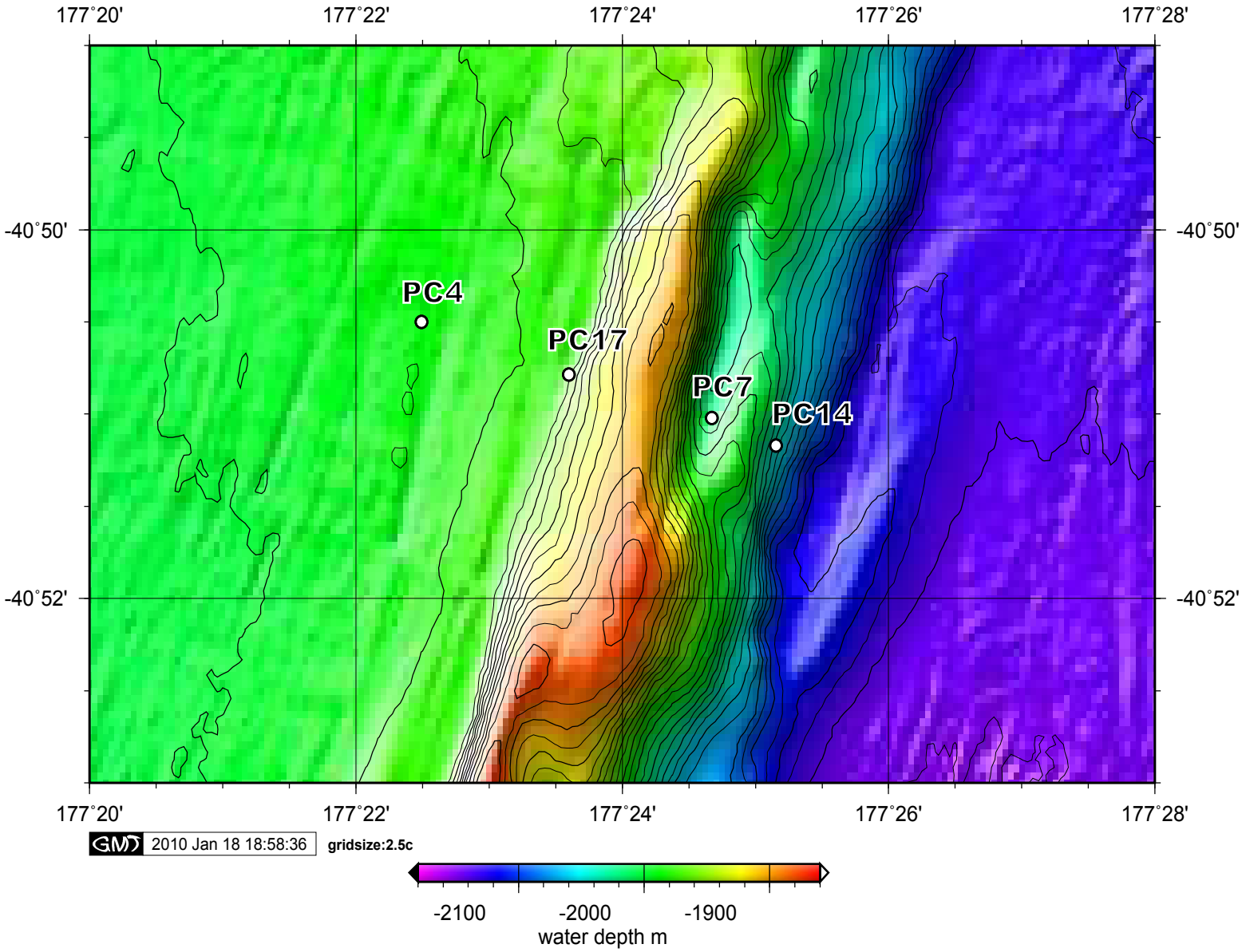
177˚20'
177˚22'
177˚24'
177˚26'
177˚28'
-40˚50'
-40˚52'
PC4
PC17
PC7
PC14
GMT 2010 Jan 18 18:58:36
gridsize:2.5c
-2100
-2000
-1900
water depth m

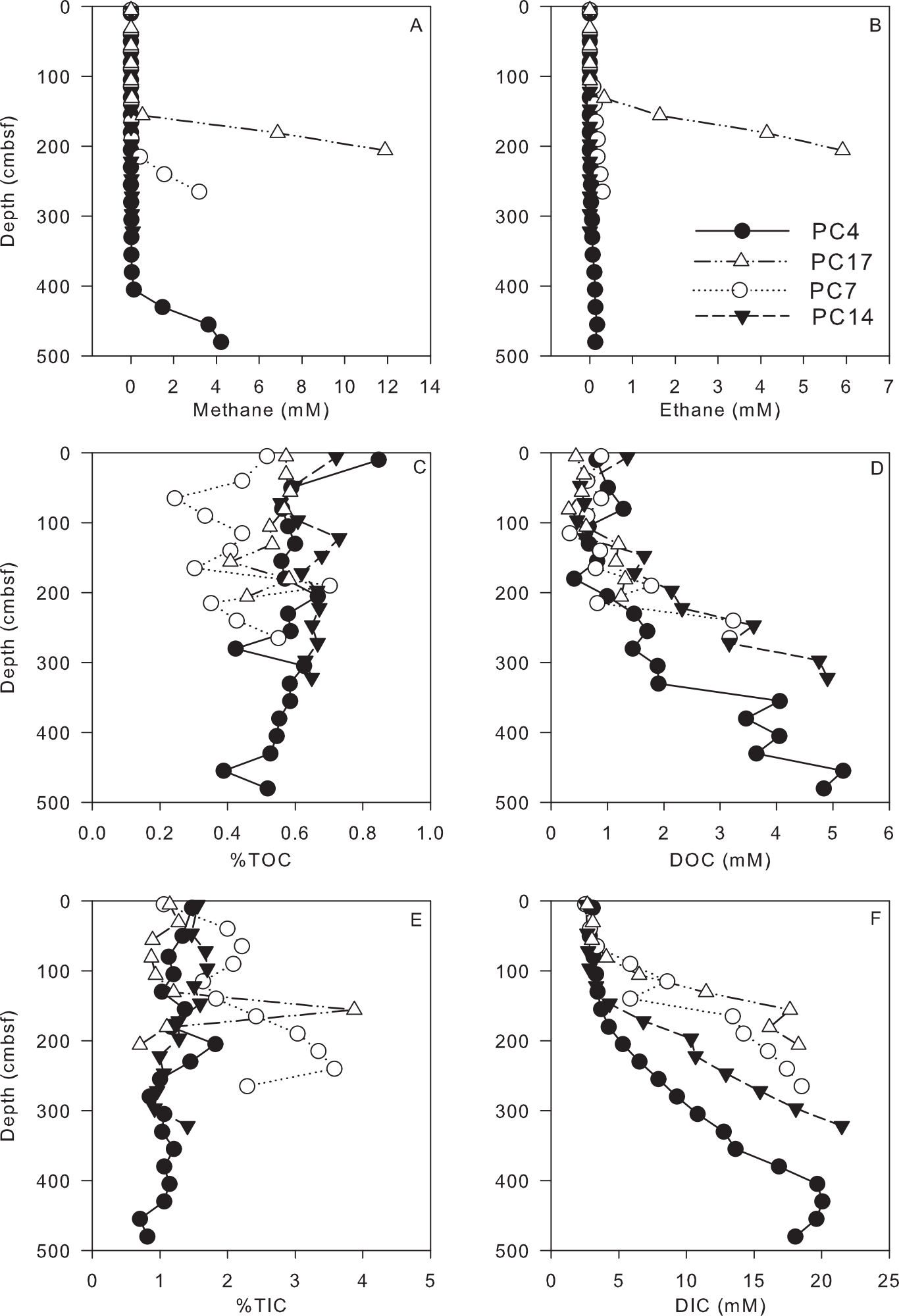
A
B
C
D
E
F
Depth (cmbsf)
Methane (mM)
Ethane (mM)
%TOC
DOC (mM)
%TIC
DIC (mM)
PC4
PC17
PC7
PC14

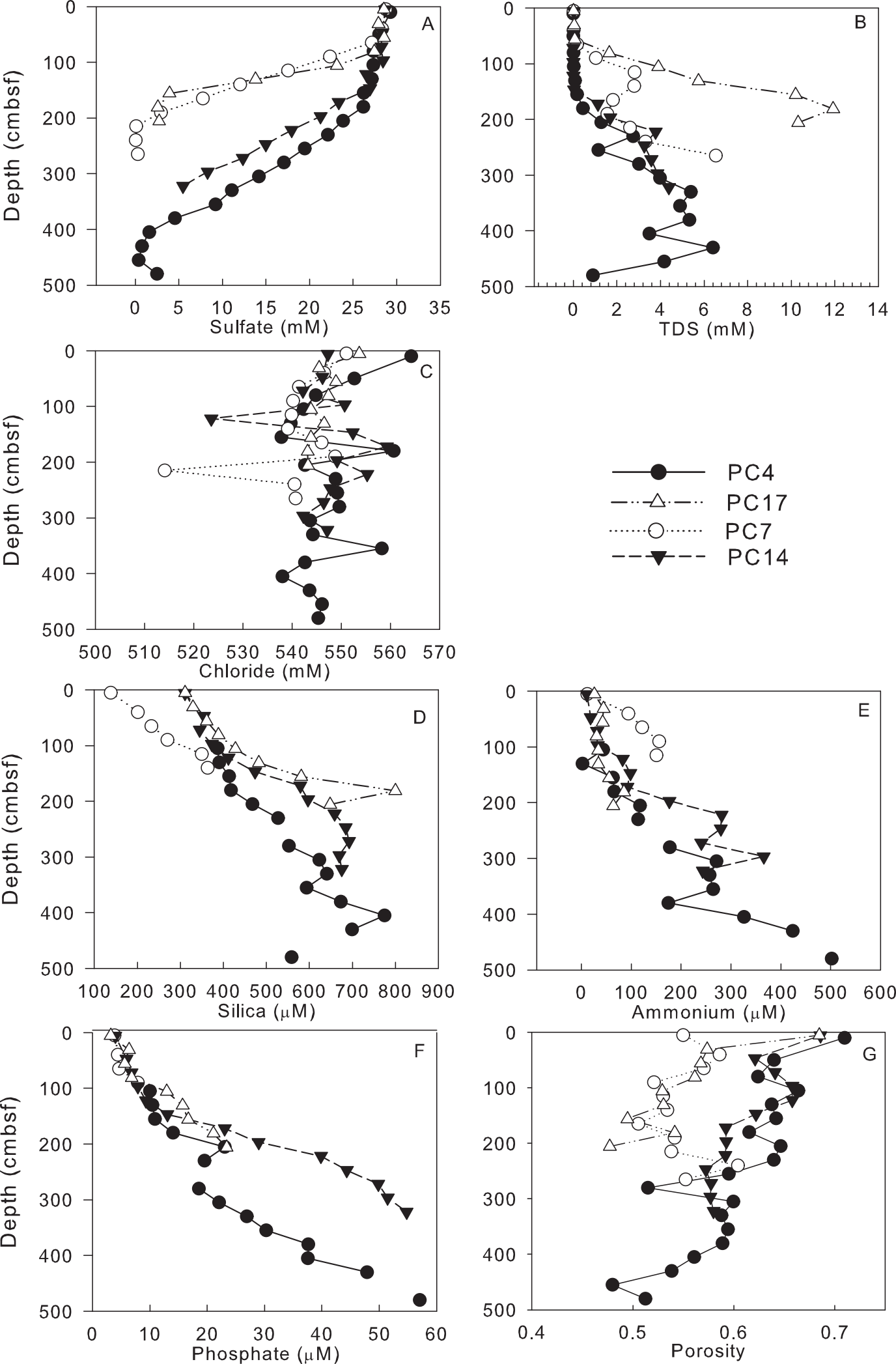
A
Depth (cmbsf)
Sulfate (mM)
B
TDS (mM)
C
Chloride (mM)
PC4
PC17
PC7
PC14
D
Silica (μM)
E
Ammonium (μM)
F
Phosphate (μM)
G
Porosity

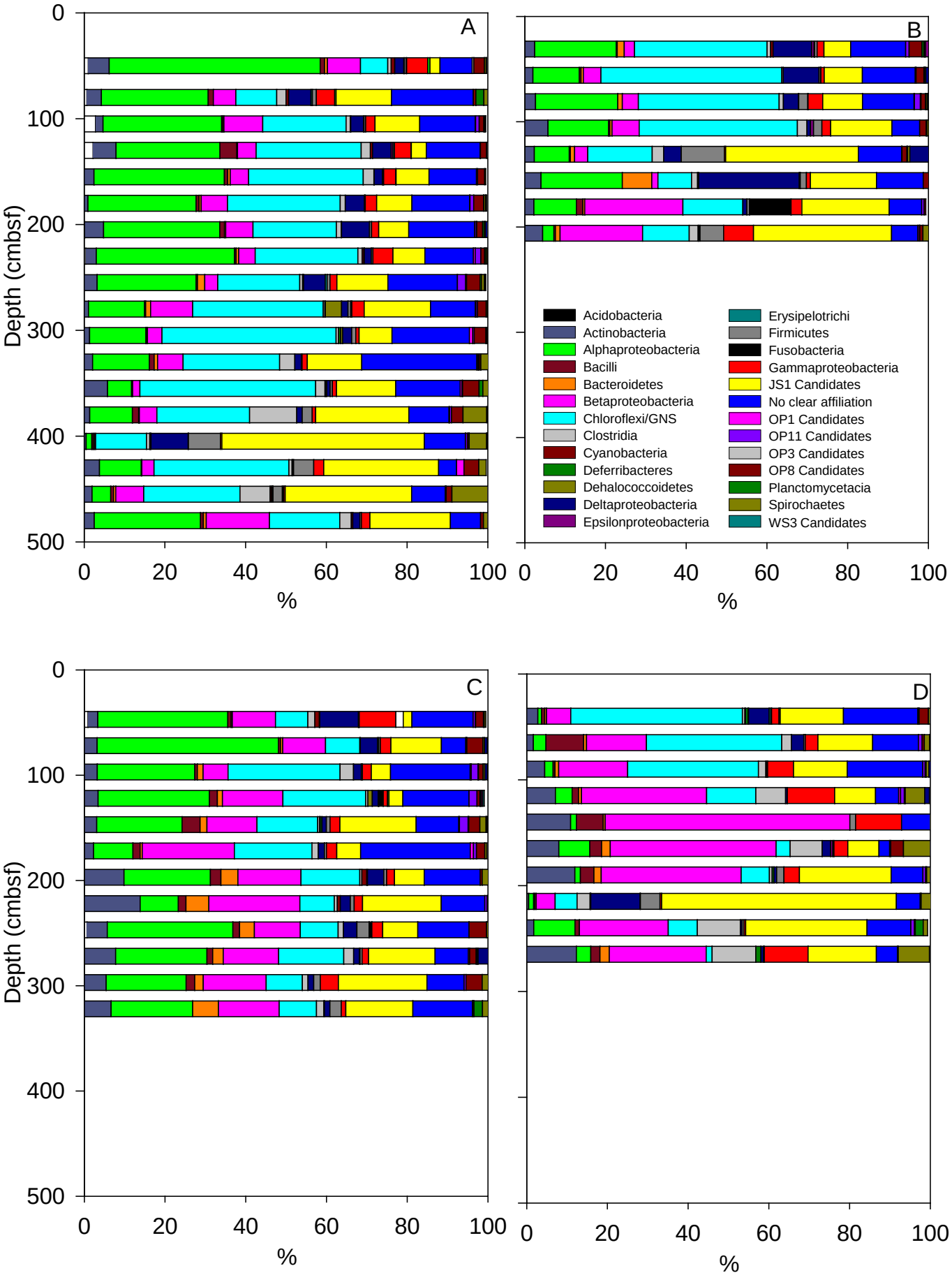
A
B
C
D
Depth (cmbsf)
0
100
200
300
400
500
0
20
40
60
80
100
%
Acidobacteria
Actinobacteria
Alphaproteobacteria
Bacilli
Bacteroidetes
Betaproteobacteria
Chloroflexi/GNS
Clostridia
Cyanobacteria
Deferribacteres
Dehalococcoidetes
Deltaproteobacteria
Epsilonproteobacteria
Erysipelotrichi
Firmicutes
Fusobacteria
Gammaproteobacteria
JS1 Candidates
No clear affiliation
OP1 Candidates
OP11 Candidates
OP3 Candidates
OP8 Candidates
Planctomycetacia
Spirochaetes
WS3 Candidates

Figure 5

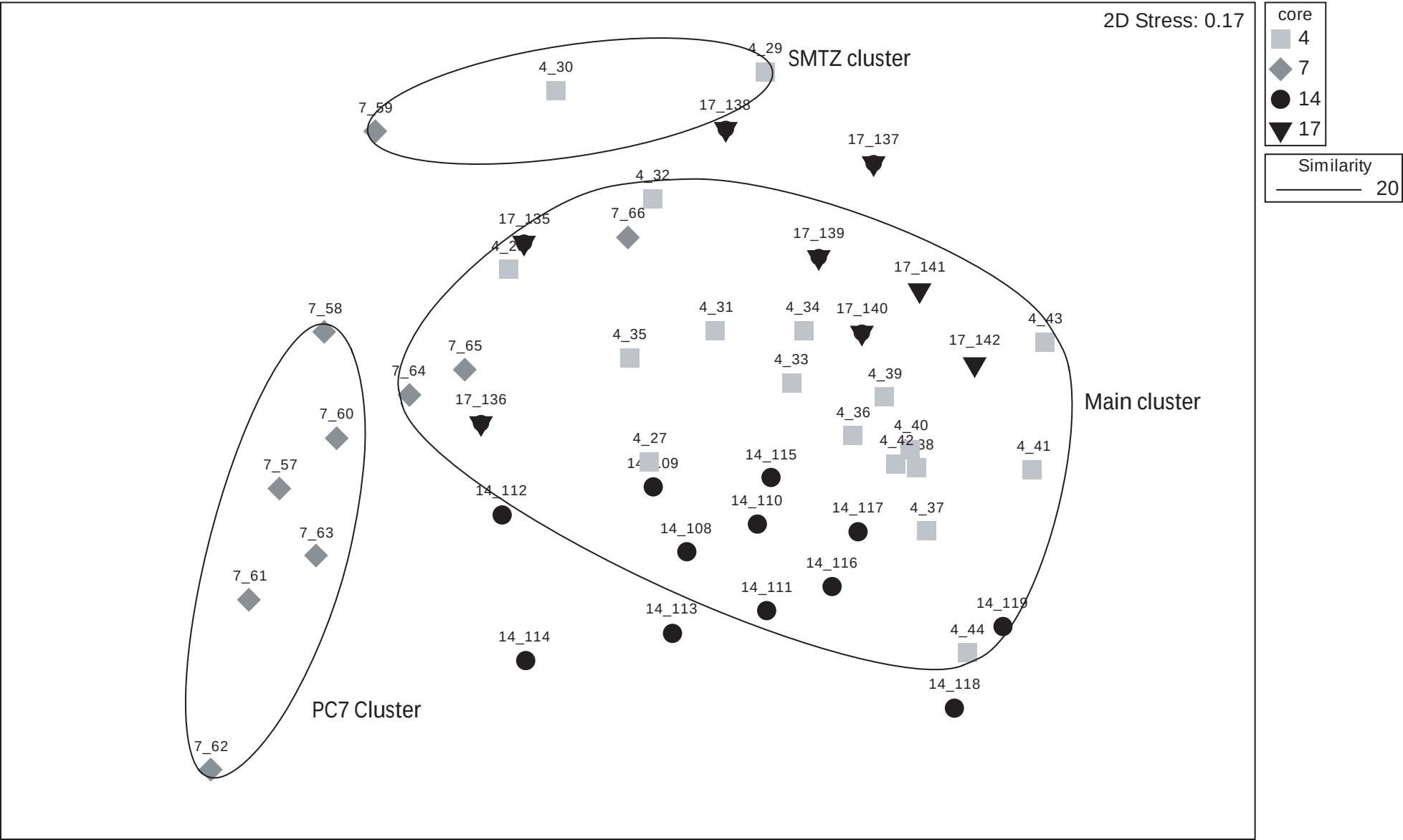
Resemblance: S17 Bray Curtis similarity
2D Stress: 0.17
core
4
7
14
17
Similarity
20
SMTZ cluster
Main cluster
PC7 Cluster
4_29
4_30
7_59
17_138
17_137
4_32
17_135
7_66
17_139
17_141
7_58
4_31
4_34
17_140
4_43
4_35
7_65
17_142
7_64
4_33
4_39
17_136
7_60
4_36
4_40
4_27
4_42
4_41
14_115
7_57
14_112
14_110
14_117
4_37
7_63
14_108
7_61
14_116
14_111
14_119
14_113
4_44
14_114
14_118
7_62